Journal of Power Sources 194 (2009) 568–573

Contents lists available at ScienceDirect

Journal of Power Sources

journal homepage: www.elsevier.com/locate/jpowsour

# Application of mesoporous carbon to counter electrode for dye-sensitized solar cells

Guiqiang Wang*, Wei Xing, Shuping Zhuo*

*School of Chemical Engineering, Shandong University of Technology, Zhangzhou Road, Zibo 255049, China*

ARTICLE INFO

*Article history:*
Received 25 December 2008
Received in revised form 12 March 2009
Accepted 23 April 2009
Available online 3 May 2009

*Keywords:*
Mesoporous carbon
Counter electrode
Dye-sensitized solar cells

ABSTRACT

The mesoporous carbons were prepared by the carbonation of the triblock copolymer F127/phloroglucinol-formaldehyde composite self-assembled in an acid medium and employed as the catalyst for triiodide reduction in dye-sensitized solar cells (DSCs). The characteristics of mesoporous carbon were analyzed by scanning electron microscopy, transmission electron microscopy, $N_2$ sorption measurement and X-ray diffraction. The mesoporous carbon with low crystallinity exhibited Brunauer–Emmett–Teller surface area of 400 $m^2\,g^{-1}$, pore diameter of 6.8 nm and pore volume of 0.63 $cm^3\,g^{-1}$. The photovoltaic performances of DSCs with mesoporous carbon counter electrode were improved by increasing the carbon loading on counter electrode due to the charge-transfer resistance of mesoporous carbon counter electrode decreasing with the increase of the carbon loading. However, further carbon loading increase has no obvious effect on the photovoltaic performance of DSCs with carbon electrode when carbon loading exceeds 300 $\mu g\,cm^{-2}$. The overall conversion efficiency of 6.18% was obtained by DSCs composed of mesoporous carbon counter electrode with the carbon loading of 339 $\mu g\,cm^{-2}$. This value is comparable to that of DSCs with conventional platinum counter electrode.



## 1. Introduction

Dye-sensitized solar cells (DSCs) have attracted much attention and have been considered as a credible alternative to other thin-film photovoltaic cells because of their high-energy conversion efficiency and low production costs [1–3]. However, further cost reduction is necessary for practical application of DSCs in the future, in addition to the need for further increasing the efficiency [4,5]. These issues have been addressed by industrial and academic research, and several strategies have been made. The application of conductive plastic substrate to DSCs reduces the cost through mass production by employing role-to-role manufacturing system [6–8]. Organic dye was used as the substitute for expensive Ru dye to cut the cost of sensitizer [9–11].

The counter electrode is an important component of DSCs. Usually, the conducting glass sheet loaded with platinum are widely used as the counter electrode for DSCs to reduce overpotential for reduction of triiodide in redox electrolyte [12,13]. Although platinum has high catalytic activity for triiodide reduction and high stability, and the amount of platinum necessary to obtain the desire catalytic effect has been kept low (<10 $\mu g\,cm^{-2}$) by finely dispersing the platinum on the conducting substrate, it is one of the expensive component materials in DSCs, and future large solar conversion system will prefer materials that are abundantly available. Therefore, it is desirable to develop alternative cheap materials for the counter electrode which should be corrosion-inert and exhibited good catalytic activity for the reduction of triiodide ion. In recent years, several varieties of carbonaceous materials such as carbon black [14], carbon nanotubes [15], activated carbon and graphite [16] have been employed as catalyst on conducting glass for counter electrode. Furthermore, organic ion-doped conducting polymers based on poly(3,4-ethylenedioxythiophene) were also used as the catalytic materials on conducting glass for DSCs with liquid electrolyte [17]. While the cost of conducting polymers is lower than that of platinum, poor adhesion to conducting substrate poses a long-term risk.

Mesoporous carbon (MC), due to their accessible porosity, high surface area, high electrical conductivity, high chemical, thermal and mechanical stability, are utilized as catalysis and electrode materials for different purpose such as protection of environment and improvement of energy efficiency [18,19]. Recently, some simple routes for the synthesis of MC directly from organic–organic composite prepared by self-assembling of block copolymers and carbon precursors have been reported [20,21]. The material cost of the MC counter electrode is apparently lower than that of platinum counter electrode. To take the advantage of the accessible porosity, high surface area and high electrical conductivity of MC, a novel counter electrode based on MC for DSCs was prepared.

* Corresponding authors. Tel.: +86 0533 2781664.
*E-mail addresses:* wgqiang123@163.com (G. Wang), kjc@sdut.edu.cn (S. Zhuo).

0378-7753/$ – see front matter © 2009 Elsevier B.V. All rights reserved.
doi:10.1016/j.jpowsour.2009.04.056

The photovoltaic performances of DSCs with MC counter electrode were analyzed.

## 2. Experimental

### 2.1. Preparation and characterization of MC and MC counter electrode

Triblock poly(ethylene oxide)-block-poly(propylene oxide)-block-poly(ethylene oxide) copolymer Pluronic F127 ($M_w$ = 12,600) was purchased from BASF Corporation. Other chemicals were purchased form J & K Chemical Limited.

Pluronic F127 was dissolved in a mixture of water (7.8 g) and ethanol (11 g), and the phloroglucinol (3.6 g) was added and stirred for 30 min. After complete dissolution of phloroglucinol, formaldehyde (3.5 g, 37 wt%) was added to the above solution and stirred for 30 min. Finally, HCl (0.1 ml, 5N) was added as a catalyst to the solution. This mixture was stirred at 30 °C for 2 h, and then heated at 100 °C in the oven for 8 h in order to promote the polymerization between phloroglucinol and formaldehyde. The resulted samples was carbonized under a nitrogen atmosphere by stepwise heating at 400 and 800 °C for 3 h, respectively. The heating rate is 1 °C $min^{-1}$. Finally, MC was obtained.

MC powder was obtained by grounding the MC sample in planetary ball milling (QM-WX4, Nanjing University Instrument Plant). To obtain the MC paste, 150 mg of MC powder was ground in a mortar with 0.2 ml $TiO_2$ colloid (10 wt%), 0.3 ml $H_2O$ and 0.1 ml 10% Triton X-100 aqueous solution. MC electrode was prepared by coating the carbon paste on fluorine-doped tin oxide (FTO) glass by doctor-blade method and then heated at 400 °C for 20 min.

Nitrogen sorption measurements were performed using ASAP-2010 (Micromeritrics, USA) at 77 K. The samples were degassed at 200 °C for 2 h before measurement. Specific surface area was calculated by the Brunauer–Emmett–Teller (BET) method using adsorption data, and the pore size distribution was determined by analyzing the adsorption branch using Barrett–Joyner–Halenda (BJH) method. S-4300 model scanning electron microscopy (Hitachi Corp.) was used for the SEM measurements. The transmission electron microscope (TEM) image was obtained by using a Hitachi H-800 transmission electron microscopy. X-ray diffraction (XRD) measurements were performed on a Rigaku D/max B diffractometer using Cu Kα radiation.

Electrochemical impedance spectroscopy (EIS) measurements were performed in a symmetric thin-layer cell consisted of two MC electrodes holding at constant space by a 20 μm thick Surlyn film (supplied by Dupont). The thin-layer cell was filled with the electrolyte containing 0.5 M KI/0.05 M $I_2$ in the mixture of ethylene carbonate (EC) and propylene carbonate (PC) (EC:PC = 8:2 by volume). The SOLARTRON SI 1287 electrochemical interface equipped with a SOLARTRON 1255B frequency response analyzer was used in the measurements.

### 2.2. Photovoltaic characterization of the DSCs with MC counter electrode

The nanocrystalline $TiO_2$ electrodes were prepared by coating $TiO_2$ colloidal paste on the FTO glass using the doctor-blade method and then heated for 30 min at 450 °C in air. After cooling to 80 °C, $TiO_2$ electrodes were dipped into 0.5 mM solutions of N3 dye in ethanol for 12 h at room temperature. The DSCs were assembled by sandwiching the dye-sensitized $TiO_2$ electrode and the counter electrode with a 25 μm thick spacer. The electrolyte was injected into the cell by the capillary effect through thin gap between the two electrodes. Photocurrent–voltage performances of DSCs with MC counter electrode were measured under the illumination of the tungsten-halogen lamp at the light intensity of 100 mW $cm^{-2}$. The active cell area was 0.2 $cm^2$.

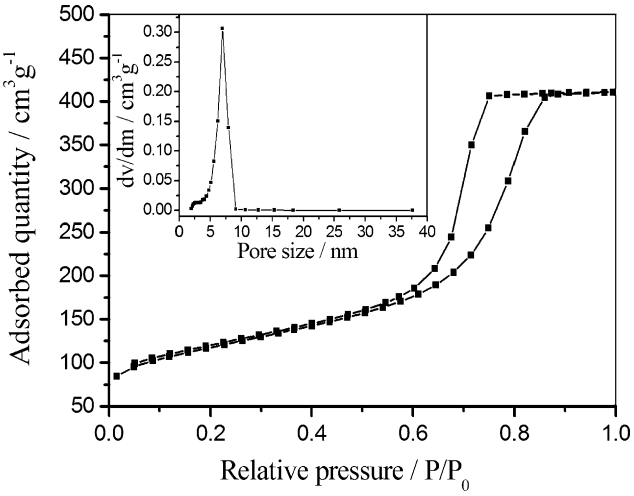


**Fig. 1.** Nitrogen sorption isotherm of MC. The inset is the corresponding BJH pore size distribution plot.

## 3. Results and discussion

### 3.1. Characteristics of MC and MC counter electrode

MC materials were prepared by the self-organization of surfactant and carbon precursors, followed by carbonization. The characteristics of MC were analyzed by nitrogen sorption measurements and TEM. The $N_2$ sorption isothermal of this materials exemplified in Fig. 1 showed IUPAC type IV pattern with H2 hysteresis loop. The hysteresis loop as a result of capillary condensation of $N_2$ inside the pores is typically ascribed to the existence of mesoporous structure in the sample. The pore size distribution curve of MC insetted in Fig. 1 indicated a narrow and well-defined pore size distribution. The specific surface area calculated by BET method and the average pore diameter calculated by BJH method were around 400 $m^2$ $g^{-1}$ and 6.8 nm, respectively. The total pore volume was about 0.63 $cm^3$ $g^{-1}$. TEM study further corroborates above analysis (Fig. 2). From Fig. 2, no long-range pore ordering was observed but instead a worm-like structure was revealed. The pore size is about 7 nm, which is consistent with the result of $N_2$ sorption measurements.

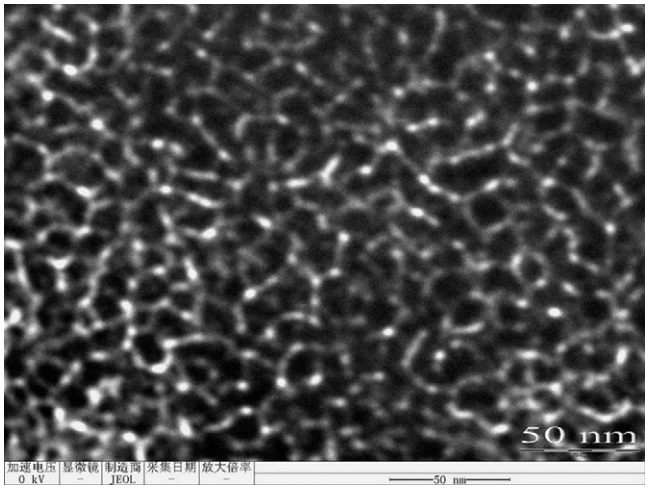


**Fig. 2.** High resolution TEM picture of MC.

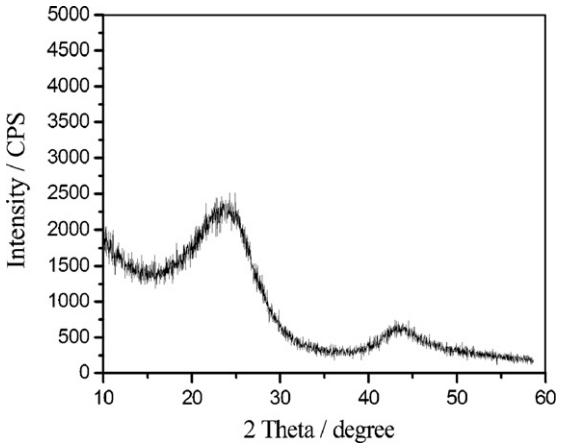


**Fig. 3.** Wide angle XRD pattern for MC.

The active sites for catalysis in the carbon materials are located at the crystal edges [14]. Consequently the carbon materials having low crystallinity and many edges may be more active than high oriented carbon materials such as the graphite and carbon nanotubes. The XRD pattern of the MC was shown in Fig. 3. The broadened peaks at 23° and 43° were observed in the XRD pattern of the MC, thereby indicating the low crystallinity of MC materials.

MC counter electrodes were prepared by coating carbon paste on FTO glass, and then heated at 400 °C. SEM image of MC layer on counter electrode was shown in Fig. 4. Based on the SEM observation, the irregular MC particle was observed (Fig. 4a), the size of the MC particle ranged from 200 nm to 1 μm. A closer observation of the MC particles revealed a wormhole-like arrangement of mesopores (Fig. 4b), which indicated that the mesoporous structure was maintained after heating at 400 °C during the preparation of MC counter electrodes.

In DSCs, the role of the counter electrode is to help the regeneration of iodide according to the reaction $I_3^- + 2e = I^-$. In the case of MC counter electrode, the reaction species, $I_3^-$, must quickly enter the pore of MC, and is reduced in the pore. Then, the regeneration species, $I^-$, must quickly diffuse out the pore. Which demand that the diameter of pore of MC must be larger than the size of $I_3^-$ and $I^-$. The size of $I_3^-$ and $I^-$ in organic solvent is about 0.5 and 0.22 nm [22], respectively. Therefore, it is apparently smaller than the size of the pore of MC.

### 3.2. Photovoltaic performances of DSCs with MC counter electrodes

The photovoltaic performances of DSCs with the MC counter electrode were measured under irradiation of 100 mW cm$^{-2}$. The photocurrent density–voltage curves of DSCs using MC electrode with various carbon loading as counter electrode were exhibited in Fig. 5. From Fig. 5, It can be seen that the cells using bare FTO conducting glass as counter electrode without any catalyst performed poorly. The short-circuit photocurrent density ($J_{sc}$), the open-circuit voltage ($V_{oc}$), the fill factor (FF) and the overall conversion efficiency ($\eta$) are 3.9 mA cm$^{-2}$, 0.493 V, 8% and 0.18%, respectively. The necessary of depositing an effective catalyst on FTO-glass can be easily appreciated from this result. The influence of the carbon loading on the short-circuit photocurrent density, the open-circuit voltage, the fill factor and the overall conversion efficiency were shown in Fig. 6. The $V_{oc}$ was hardly influenced by variation of the carbon loading on counter electrode as shown in Fig. 6b. However, the $J_{sc}$, the FF and the $\eta$ increased with the increase of the carbon loading. The carbon loading increased from 67 to 323 μg cm$^{-2}$, the $J_{sc}$, the FF and the $\eta$ of DSCs with MC counter electrode increased from

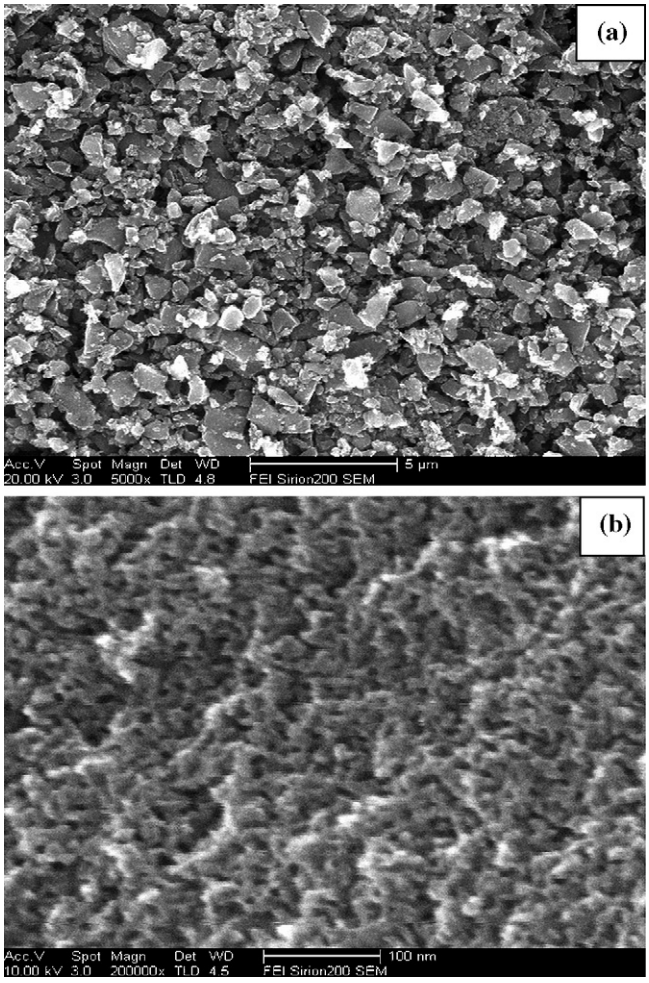


**Fig. 4.** SEM image (a) and high magnification SEM image (b) of carbon layer for MC counter electrode.

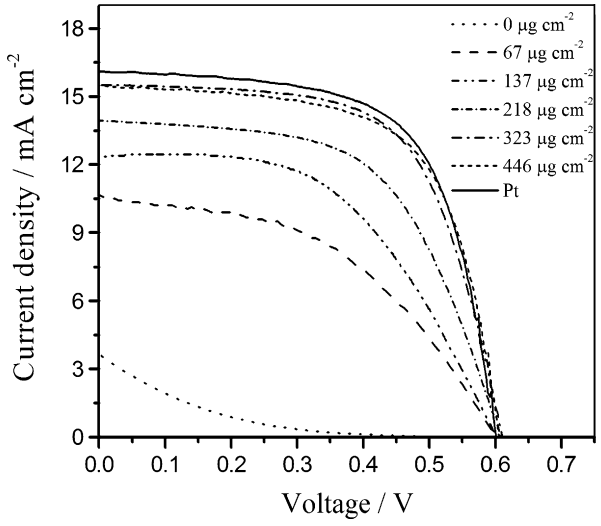


**Fig. 5.** The photocurrent–voltage curves of DSCs with the MC counter electrode measured in the electrolyte containing 0.5 M KI/0.05 M $I_2$ in the mixture of ethylene carbonate (EC) and propylene carbonate (PC) (EC:PC = 8:2 by volume). Light intensity 100 mW cm$^{-2}$, active area 0.2 cm$^2$.

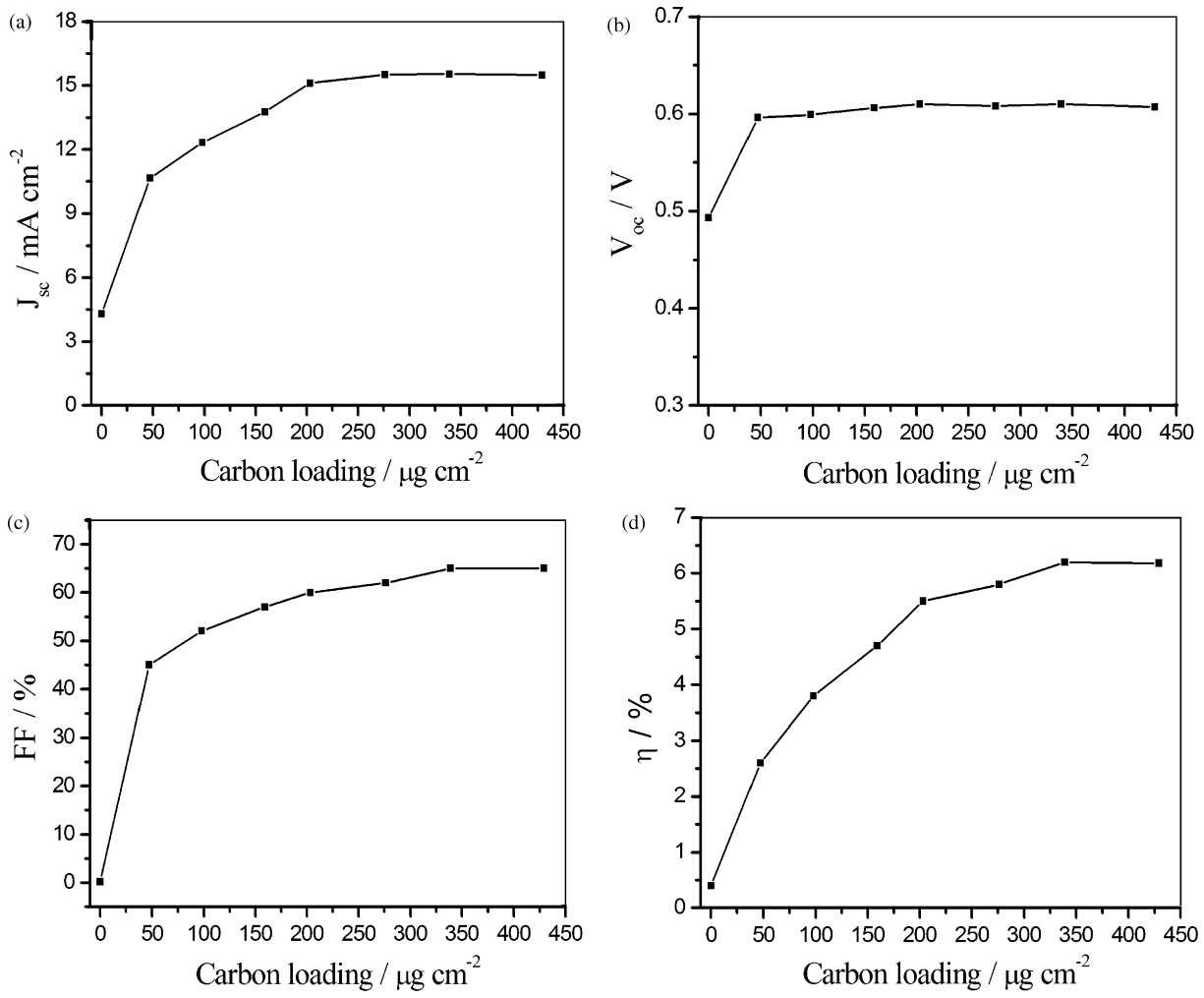


**Fig. 6.** Relations between the carbon loading on FTO glass as counter electrode and the photovoltaic performances of DSCs with MC electrode for short-circuit current (a), open-circuit voltage (b), fill factor (c) and overall conversion efficiency (d).

10.7 to 15.5 mA cm$^{-2}$, 45 to 65% and 2.60 to 6.18%, respectively. However, the photovoltaic performance of DSCs with MC counter electrode hardly changed with the increase in the carbon loading as the carbon loading exceeded 300 μg cm$^{-2}$.

The photovoltaic performance of DSCs with conventional platinum counter electrode was also shown in Fig. 5 as a comparison. Platinum counter electrodes were prepared by thermal decomposition of hexachloroplatinic acid on FTO glass. The platinum loading was about 10 μg cm$^{-2}$. The overall conversion efficiency of DSCs with platinum electrode was 6.26%. Thus, as the carbon loading exceeded 300 μg cm$^{-2}$, the photovoltaic performance of DSCs with MC counter electrode was comparable to that of the DSCs with platinum counter electrode.

To find the cause of the improvement in cell performance with the carbon loading, the charge-transfer resistance ($R_{ct}$) of the MC counter electrode which characterizes the electrocatalytic activity for the triiodide reduction was studied by applying electrochemical impedance spectroscopy. The electrochemical impedance spectra of the symmetric thin-layer cell consisted of two identical MC electrodes were shown in Fig. 7. An impedance spectrum of the cell consisted of two conventional platinum counter electrode was also shown in Fig. 7 as comparison. The equivalent circuit for this type of the cell was shown in Fig. 8 [13]. The ohmic serial resistance ($R_s$) can be determined according to the high frequency of the impendence where the phase is zero, which is composed of the sheet resistance of the two identical MC electrodes and the electrolytic resistance. Comparing with the sheet resistance of the electrode, the electrolytic resistance can be neglected. The ohmic serial resistance is then taken at two times of the sheet resistance of the measuring electrode. In the middle frequency range of 100 Hz–100 kHz, the impedance is dominated by the RC network of the MC electrode/electrolyte interface, consisting of the charge-transfer resistance ($R_{ct}$) and the capacitance of electrical double layer ($C_{DL}$). The impedance in the frequency range of 0.1–100 Hz can be attributed to the Nernst diffusion impedance. By fitting the EIS spectra using the equivalent circuit in Fig. 8, the value of $R_{ct}$ can be obtained from the diameter of the semicircle illuminated in the spectra at the high frequency region. From the spectra shown in Fig. 7, it was observed that the sheet resistance of MC electrode hardly varied with the increase in carbon loading. However, the charge-transfer resistance of MC electrode was decreased with the increase in carbon loading. The carbon loading increase from 57 to 328 μg cm$^{-2}$, the charge-transfer resistances of MC counter electrode decrease from 8 to 0.7 Ω cm$^2$. As shown in Fig. 7, the MC electrode with carbon loading of 328 μg cm$^{-2}$ exhibited same catalytic activity for triiodide reduction with conventional platinum electrode. The decreased charge-transfer resistance result the decrease of the overvoltage loss on the counter electrode, and then improve the overall cell performance.

For comparison, conventional active carbon (AC) with surface area of 780 m$^2$ g$^{-1}$ (Jiangxi Santar Co. Ltd.) was used as the catalyst for triiodide reduction to prepare the AC counter electrode. The

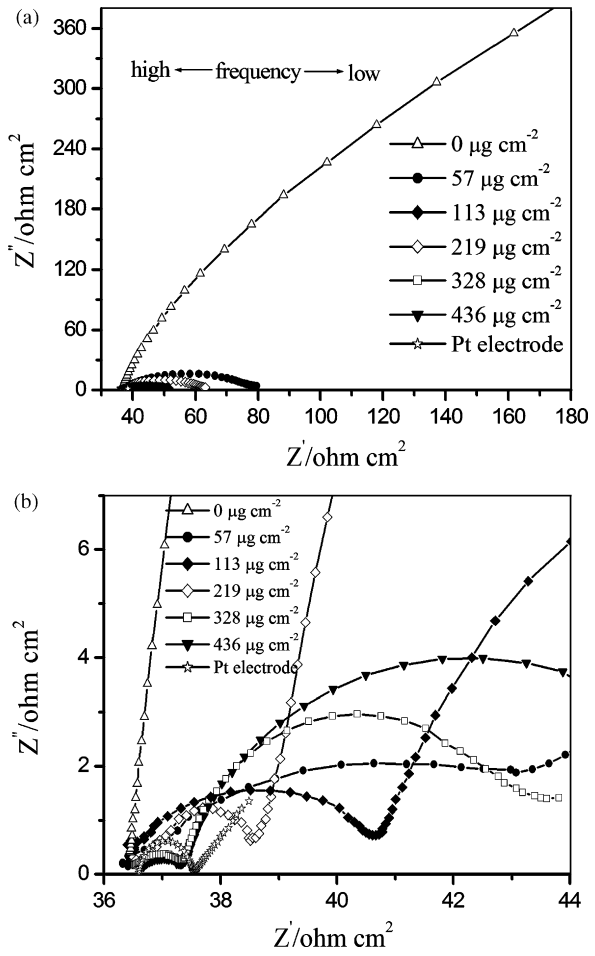


**Fig. 7.** Electrochemical impedance spectroscopy of the symmetric thin-layer cell consisted of two MC electrodes taken at zero bias, ac amplitude 5 mV, frequency range 0.1–$10^6$ Hz, the electrolyte composition was the same as that in Fig. 5 (b) was expanded range of ordinate and abscissa from (a) in high frequency region.

photovoltaic performance of DSCs with AC counter electrode was also measured. The short-circuit current density, the open-circuit voltage, the fill factor and the overall conversion efficiency of DSCs with the AC counter electrode with carbon loading of 358 mg cm$^{-2}$ were 15.1 mA cm$^{-2}$, 0.605 V, 0.55 and 5.02%, respectively. Further increase of the AC loading hardly affected the photovoltaic performance. The short-circuit current density and the open-circuit voltage of DSCs with AC counter electrode are comparable to that of DSCs with MC counter electrode, while the fill factor and the overall conversion efficiency are lower than that of DSCs with MC counter electrode. The reasons of above results may be due to the difference of porous structure between MC and AC. MC possesses large mesopores with average pore size of 7 nm, in which ionic diffusion is favorable with small hindrance. In contrast, AC with larger surface area possesses mainly micropores of less than 2 nm,

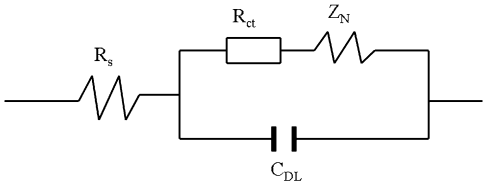


**Fig. 8.** Equivalent circuit for the electrochemical impedance spectra in Fig. 7. $Z_N$: Nernst diffusion impedance; $R_{ct}$: charge-transfer resistance; $C_{DL}$: capacitance of electric double layer; $R_s$: ohmic serial resistance.

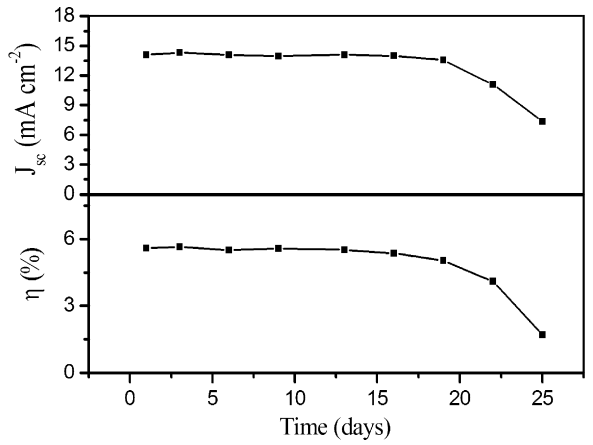


**Fig. 9.** Variation of the short-circuit current and the overall conversion efficiency of DSCs with time in continuous illumination with light of 100 mW cm$^{-2}$.

which increase the diffusion resistance of redox couple $I^-/I_3^-$ in its pore channel, thus increasing the series resistance of the cell. The increased series resistance directly deteriorates the fill factor and the over-all conversion efficiency of DSCs.

The stability of DSCs based on the MC counter electrodes was studied under continuous illumination by monitoring the photocurrent–voltage characteristics with time. The results were shown in Fig. 9. It can be seen that the short-circuit photocurrent density and the cell efficiency were almost unchanged during test within 2 weeks. The reduction of the cell performance observed after 2 weeks can be attribute the leakage of liquid electrolyte caused by the difficulty of cell sealing. Further study on the cell sealing and on the stability of the cell with MC counter electrode are in the progress.

## 4. Conclusions

MC with a specific surface area of 400 m$^2$ g$^{-1}$, pore diameter of 6.8 nm and pore volume of 0.63 cm$^3$ g$^{-1}$ were employed as catalyst for triiodide reduction on FTO glass used as counter electrodes in dye-sensitized solar cells. MC electrode exhibited high electrocatalytic activity for triiodide reduction due to low crystallinity of mesoporous carbon. The short-circuit current density, the fill factor and the overall conversion efficiency of DSCs with MC counter electrode were improved by increasing the carbon loading in range of 0–300 μg cm$^{-2}$. When the carbon loading exceeded 300 μg cm$^{-2}$, the overall conversion efficiency of 6.18% was obtained. This result is comparable to that of DSCs with conventional platinum electrode.

## Acknowledgements

This work was supported by the Natural Science foundation of china (No. 20773082) and the Department of Science and Technology of Shandong (No. 2006BS09003).

## References

[1] B. O'Regan, M. Grätzel, Nature 353 (1991) 737–739.
[2] M.K. Nazeeruddin, A. Kay, I. Rodicio, R. Humphry-Baker, E. Mueller, P. Liska, N. Vlachopoulos, M. Grätzel, J. Am. Chem. Soc. 115 (1993) 6382–6390.
[3] M. Grätzel, J. Photochem. Photobiol. A 164 (2004) 3–14.
[4] S. Ito, P. Liska, P. Comte, R. Charvet, P. Pechy, U. Bach, L. Shumit-Mende, S.M. Zakeeruddin, A. Kay, M.K. Nazeeruddin, M. Grätzel, Chem. Commun. 20 (2005) 4351–4353.
[5] A. Kay, M. Grätzel, Sol. Energy Mater. Sol. Cells 44 (1996) 99–117.
[6] H. Lindstrom, A. Holmberg, E. Magnusson, S.E. Lindquist, L. Malmqvist, A. Hagfeldt, Nano. Lett. 1 (2001) 97–100.
[7] T.N. Murakami, Y. Kijitori, N. Kawashima, T. Miyasaka, J. Photochem. Photobiol. A 164 (2004) 187–191.

[8] M. Dürr, A. Schmid, M. Obermaier, S. Rosselli, A. Yasuda, G. Nelles, Nat. Mater. 4 (2005) 607–611.
[9] H. Hara, T. Sato, R. Katoh, A. Furube, Y. Ohga, A. Shinpo, S. Suga, K. Sayama, H. Arakawa, J. Phys. Chem. B 107 (2003) 597–606.
[10] D.P. Hagberg, T. Edvinsson, T. Marinado, G. Boschloo, A. Hagfeldt, L. Sun, Chem. Commun. 21 (2006) 2245–2247.
[11] H. Qin, S. Wenger, M. Xu, F. Gao, P. Wang, M. Grätzel, J. Am. Chem. Soc. 130 (2008) 9202–9203.
[12] N. Papageorgiou, W.F. Maier, M. Grätzel, J. Electrochem. Soc. 144 (1997) 876–907.
[13] A. Hauch, A. Georg, Electrochim. Acta 46 (2001) 3457–3466.
[14] T.N. Murakami, S. Ito, Q. Wamg, M.K. Nazeeruddin, T. Bessho, I. Cesar, P. Liska, R. Humphry-Baker, P. Comte, M. Grätzel, J. Electrochem. Soc. 153 (2006) A2255–A2261.
[15] K. Suzuki, M. Yamamoto, M. Kumagai, S. Yanagida, Chem. Lett. 32 (2003) 28–29.
[16] K. Imoto, K. Takatashi, T. Yamaguchi, T. Komura, J. Nakamura, K. Murata, Sol. Energy Mater. Sol. Cells 79 (2003) 459–469.
[17] Y. Saito, W. Kuto, T. Kitamura, Y. Wada, S. Yanagida, J. Photochem. Photobiol. A 164 (2004) 155–157.
[18] F. Su, J. Zeng, X. Bao, Y. Yu, J. Lee, X. Zhao, Chem. Mater. 17 (2005) 3960–3967.
[19] W. Xing, S. Qiao, R. Ding, F. Li, G. Lu, Carbon 44 (2006) 216–224.
[20] F. Zhang, Y. Meng, D. Gu, Y. Yan, C. Yu, B. Tu, J. Am. Chem. Soc. 127 (2005) 13508–13509.
[21] C. Liu, L. Li, H. Song, X. Chen, Chem. Commun. 22 (2007) 757–759.
[22] H. Sakane, T. Mitsui, H. Tanida, I. Watanabe, J. Synchrotron Radiat. 8 (2001) 674–676.